ERDC/CERL TR-24-1

**US Army Corps
of Engineers®**
Engineer Research and
Development Center

Navigation Systems Research Program (NAVSYS)

Simulated Barge Impacts on Fiber-Reinforced Polymers (FRP) Composite Sandwich Panels

Dynamic Finite Element Analysis (FEA) to Develop Force Time Histories to Be Used on Experimental Testing

Anthony Perez-Rivera, Jonathan C. Trovillion,
Peter B. Stynoski and Jeffrey P. Ryan

January 2024

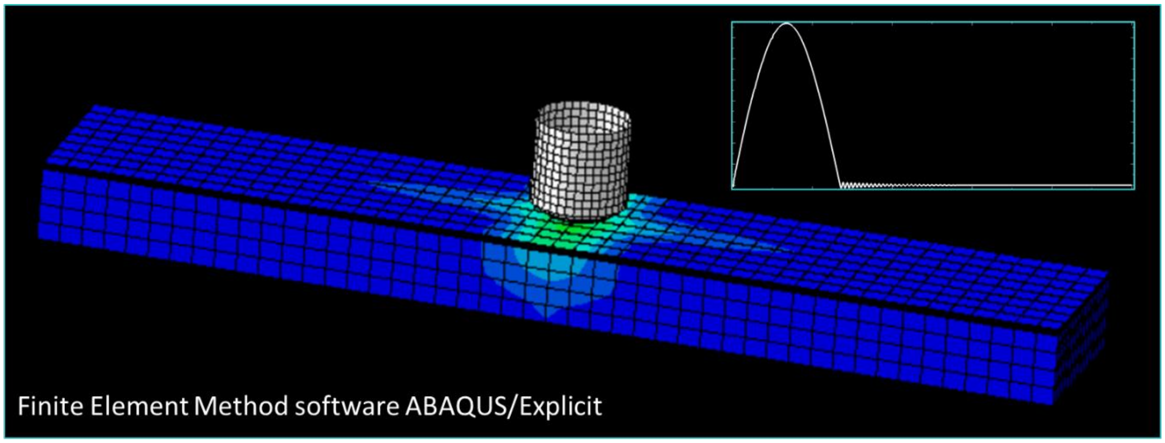

Finite Element Method software ABAQUS/Explicit

Construction Engineering
Research Laboratory

Navigation Systems Research Program
(NAVSYS)

ERDC/CERL TR-24-1
January 2024

Simulated Barge Impacts on Fiber-Reinforced Polymers (FRP) Composite Sandwich Panels

Dynamic Finite Element Analysis (FEA) to Develop Force Time Histories to Be Used on Experimental Testing

Anthony Perez-Rivera, Jonathan C. Trovillion, Peter B. Stynoski and Jeffrey P. Ryan

US Army Engineer Research and Development Center (ERDC)
Construction Engineering Research Laboratory (CERL)
2902 Newmark Drive
Champaign, IL 61822

Final Report

Prepared for US Army Engineer Research and Development Center (ERDC)
Construction Engineering Research Laboratory (CERL)
Champaign, IL 61822

Under “Composite Materials for Sector Gates and Vertical Lift Gates.” AMSCO 031391; Funding Account U4375150

Abstract

The purpose of this study is to evaluate the dynamic response of fiber-reinforced polymer (FRP) composite sandwich panels subjected to typical barge impact masses and velocities to develop force time histories that can be used in controlled experimental testing. Dynamic analyses were performed on FRP composite sandwich panels using the finite element method software Abaqus/Explicit. The "traction-separation" law in the Abaqus software is used to define the cohesive surface interaction properties to evaluate the damage between FRP composite laminate layers as well as the core separation within the sandwich panels. Numerical models were developed to better understand the damage caused by barge impacts and the effects of impacts on the dynamic response of composite structures. Force, displacement, and velocity time histories were obtained with finite element modeling for several mass and velocity cases to develop experimental testing procedures for these types of structures.

Contents

Figures and Tables

Figures

Tables

Preface

This study was conducted for the US Army Engineer Research and Development Center (ERDC), Construction Engineering Research Laboratory (CERL), under the work unit, “Composite Materials for Sector Gates and Vertical Lift Gates” (AMSCO 031391, Funding Account U4375150). The technical monitor was Mr. Jonathan Trovillion (ERDC-CERL).

The work was performed by the Materials and Structures Branch of the Infrastructure Science and Engineering Division, US Army ERDC-CERL. At the time of publication, Ms. Danielle Williams was branch chief, Mr. Timothy Shelton was division chief, and Dr. Justin Berman was the technical director for Infrastructure Science and Engineering. The deputy director of ERDC-CERL was Ms. Michelle Hanson, and the director was Dr. Andrew Nelson.

The authors gratefully acknowledge, in alphabetical order, the assistance and guidance of several teammates who were not available to extend their contributions as authors. Ms. Heather Gathman performed literature review for indenter scaling and drafted the initial test fixture design. Mr. John Harper generated an initial experiment design and provided material properties to be used on finite element analysis.

COL Christian Patterson was the commander of ERDC, and Dr. David W. Pittman was the director.

1 Introduction

1.1 Background

As the use of fiber reinforced polymer (FRP) composites as structural materials evolves, the United States Army Corps of Engineers (USACE) has studied the functionality, durability, and structural integrity of these materials in civil works infrastructure. FRP composites have advantages such as high mechanical strength with respect to their density and excellent resistance to environmental degradation compared to traditional construction materials like steel. Several analytical and experimental tests have been conducted by USACE to understand structural behavior due to barge impacts. A full-scale field test was conducted at Winfield Lock and Dam, where a scaling of an existing impact force time history was recorded (Ebeling et al. 2010). Even considering previous efforts and experiments made by USACE, there is limited research about the dynamic response of FRP composite sandwich panels subjected to typical barge impact masses and velocities. Detailed finite element analyses employing damage caused by a barge impact and its effect on the dynamic response of composite structures are analytical tools implemented to better understand these types of structures.

1.2 Objectives

This effort intends to improve our understanding of the damage caused by barge impacts and impact effects on the dynamic response of FRP composite structures. The main objective is to use finite element modeling (FEM) to obtain force, displacement, and velocity time histories that will be used for experimental testing procedures for these types of structures. Time histories are developed for several mass and velocity cases representing scaled and real-world case scenarios for barges.

1.3 Approach

The proposed effort evaluates the dynamic response of FRP composite sandwich panels subjected to typical barge impact masses and velocities to develop force time histories to be used in controlled experimental testing. This effort includes the use of Abaqus/Explicit, which is commercially available, nonlinear finite element software. To evaluate the damage between FRP composite laminate layers as well core separation in the sandwich panels, the “traction-separation” law available in the Abaqus software is used to incorporate cohesive interaction properties.

1.4 Research Significance

This effort contributes time history estimates obtained with FEM. Immediate transfer of technology will result in the installation of a composite vertical lift gate structure at the W. P. Franklin Dam in Florida. This contribution could improve navigation infrastructure by enabling the use of composite materials rather than conventional materials such as steel.

W. P. Franklin is a 103.63 m (340 ft) spillway with eight vertical lift gates (See Figure 1).[*] Gate dimensions are 11.83 m (38.8 ft) × 5.85 m (19.2 ft) (assembled from two pieces) with a weight of approximately 21,772 kg (48,000 lb). Gates can see approximately 1.52 m (5 ft) of hydraulic head in the closed position on either side of the gate (normal and reverse head) depending on water conditions.

Figure 1. W. P. Franklin Spillway vertical lift gates, Okeechobee Waterway, Florida. (US Army Corps of Engineers, Jacksonville District. n.d. Media. Images. Accessed 2023. https://www.saj.usace.army.mil/Media/Images/igphoto/2001724853/. Public domain.)

---

[*] For a full list of the spelled-out forms of the units of measure and the unit conversions used in this document, please refer to *US Government Publishing Office Style Manual*, 31st ed. (Washington, DC: US Government Publishing Office, 2016), 248–52, 345–47, https://www.govinfo.gov/content/pkg/GPO-STYLEMANUAL-2016/pdf/GPO-STYLEMANUAL-2016.pdf.

1.5 Overview

Chapter 2 presents the geometry, properties, and typical layouts of FRP wicket gates and orthotropic properties that are assigned in the FEM of these type of structures. Chapter 3 presents the cohesive interaction properties used to predict FRP interface delamination. Chapter 4 includes a brief review of previous barge impact experiments. It also presents typical barge velocities, approach angles, and impact loads. Chapter 5 presents the geometry, properties, and typical layups of the FRP composite sandwich panels to be used for FEM and experiments. Details of the numerical models developed in this investigation are presented in Chapter 6. Conclusions and recommendations for further studies are presented in Chapter 7.

2 Fiber-Reinforced Polymers (FRP) Wicket Gate Modeling

2.1 Introduction

This chapter presents the geometry, properties, and typical layouts of FRP wicket gates that were experimentally tested. The focus of this chapter is to show how orthotropic properties are used to simulate composite material behavior and how these are assigned in FEM by using engineering constants. Several experiments were conducted at West Virginia University by Vijay et al. (2016), and the obtained results were used to validate finite element (FE) models performed at the Construction Engineering Research Laboratory (CERL).

2.2 Samples Geometry

The FRP wicket gates length, width, and thickness dimensions were 5.03 m (198 in.), 1.17 m (46 in.), and 0.227 m (9 in.), respectively. There were 14 webs across the 1.17 m wide section of the wicket gate, with top and bottom flange thicknesses of 13.28 mm (0.523 in.) each, and web thicknesses of 10.16 mm (0.4 in.) each. Typical primary and secondary web dimensions obtained from Vijay et al. (2016) are 10.16 mm (0.4 in.) at 89 mm (3.5 in.) C-C and 3.1 mm (0.12 in.) at 105 mm (4.13 in.) C-C, respectively. Figure 2 shows the FRP wicket gate FEM.

Figure 2. Fiber-reinforced polymers (FRP) wicket gate finite element modeling (FEM).

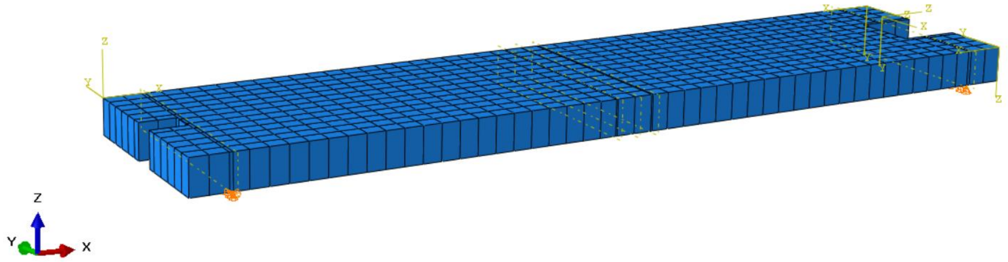

2.3 Sample Material Properties

Wicket gate face skins and webs consisted of highly directional E-glass fabrics with fibers running primarily in the 0° direction along the length of the gate for resisting bending loads and triaxial fabrics with fibers in the ±45°and 90° directions for resisting in-plane shear and transverse forces, respectively. The fiber and fabric layup of the top and bottom face sheets were symmetric to the midsurface. Foam was used to fill the hollow core cavities between webs. Wicket gate face skin and core material properties were obtained from experiments conducted at West Virginia University by Vijay et al. (2016) and are summarized in Table 1.

Table 1. FRP wicket gate properties.

Part	E_1 MPa (ksi)	E_2 MPa (ksi)	E_3 MPa (ksi)	v_{12}	v_{13}	v_{23}	G_{12} MPa (ksi)	G_{13} MPa (ksi)	G_{23} MPa (ksi)
FRP Skin	28,269 (4,100)	15,168 (2,200)	15,168 (2,200)	0.38	0.38	0.38	3,282 (476)	3,282 (476)	3,282 (476)
Primary Web	28,269 (4,100)	16,547 (2,400)	16,547 (2,400)	0.38	0.38	0.38	3,082 (447)	3,082 (447)	3,082 (447)
Secondary Web	23,442 (3,400)	17,926 (2,600)	17,926 (2,600)	0.38	0.38	0.38	3,778 (548)	3,778 (548)	3,778 (548)

2.4 FRP Wicket Gate Experiments

An FRP wicket gate was proof loaded in three-point bending over a span of 4.57 m (15 ft) with a load of 89 kN (20,000 lb) applied against a beam of 228 mm (9 in.) width. The vertical deflection measured at the center of the span for the maximum load of 89 kN was 14.81 mm (0.583 in.). Refer to Vijay et al. (2016) for the experimental set up of the proof loading test.

2.5 FRP Wicket Gate Finite Element (FE) Models

The FRP wicket gate three-point bending test was modeled by using the static finite element method in Abaqus/Standard. Three different parts were created and later assembled together: (1) face sheet, (2) primary webs, and (3) secondary webs. These parts were created by using 3D-deformable shell elements (S4R) with the orthotropic properties assigned in the model using engineering constants. For simplicity, the material properties of the foam cores were neglected. Similar to the experiment, a span of 4.57 m (15 ft) with a load of 89 kN (20,000 lb) was applied for a 228 mm (9 in.) width. A convergence study was performed to determine the mesh seed size, resulting in a 25.4 mm (1 in.) seed size. Load and displacement boundary conditions as well as mesh seed size are shown in Figure 3.

Figure 3. FRP wicket gate: (*a*) finite element (FE) boundary conditions and (*b*) mesh seed size.

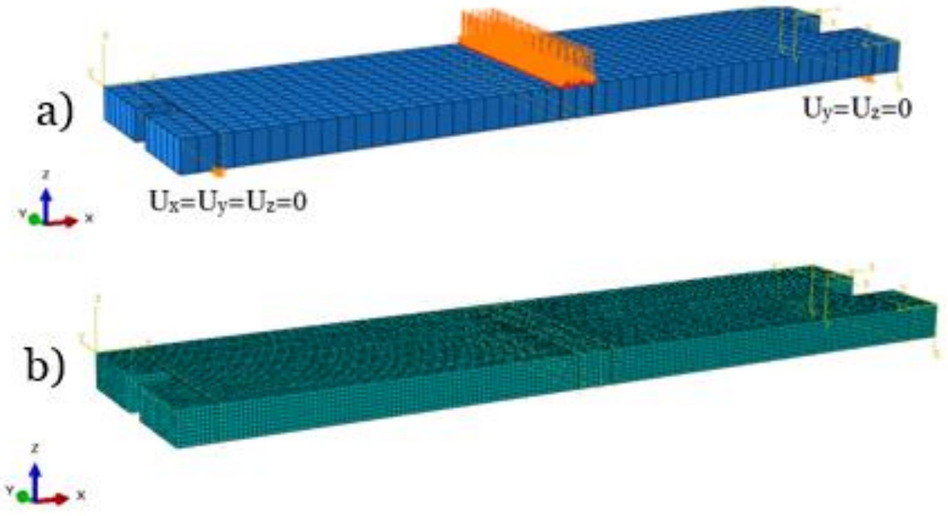

2.6 FRP Wicket Gate Results

FRP wicket gate experiment and FE model results are compared in Figure 4. Load-deflection curves from FE models are in very good agreement with the experiment. The FE model vertical deflection measured at the center of the span for the maximum load of 89 kN (20 kips) was 14.58 mm (0.574 in.) with about a 1.5% difference when compared to the experimental displacement. It can be concluded that the FE models with orthotropic properties obtained by using engineering constants in Abaqus could result in close approximations. These types of properties will be used in later chapters of this report.

Figure 4. Load vs. deflection (experiment by Vijay et al. 2016 vs. Construction Engineering Research Laboratory's [CERL] finite element modeling [FEM] in Abaqus).

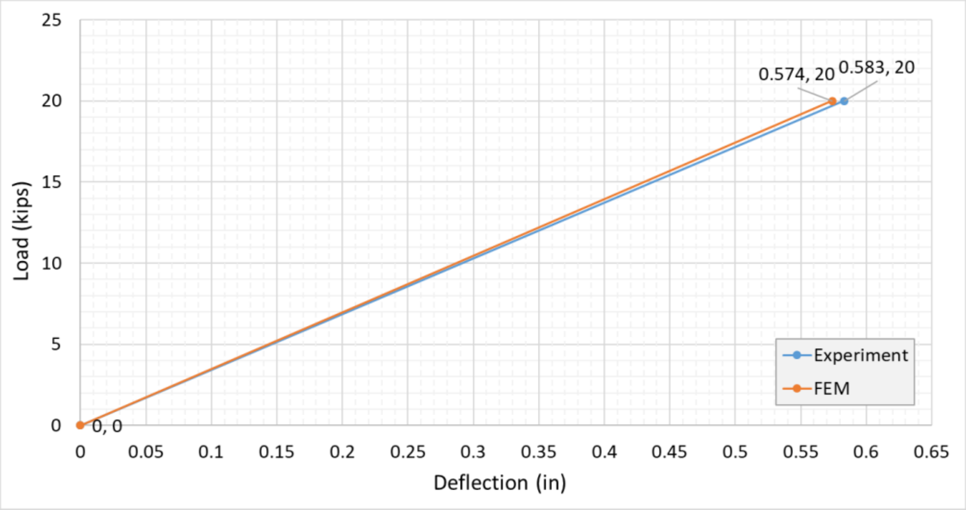

3 FRP Cohesive Interaction Properties

3.1 Introduction

This chapter presents how cohesive interaction properties can be used to simulate FRP interface delamination in FE models. To predict FRP interface delamination, cohesive interaction properties were assigned in FE models by using the traction–separation law available in Abaqus (2017). FE models of this study were created when experiments to obtain cohesive interaction properties were not conducted yet for the FRP composite sandwich panels available at CERL. Because of this reason, experiments and FE models obtained from literature were replicated in house at CERL to study the cohesive interaction properties and how these can be implemented in FE models. In the absence of experimental data for the samples available at CERL, the cohesive interaction properties discussed in this chapter are used in Chapters 5 and 6.

3.2 Cohesive Interaction Properties

Interaction properties between layers are assigned using the traction–separation law (Abaqus 2017). To use the traction-separation law, it is required to define the stiffness terms (K_n, K_s, and K_t), the damage initiation contact stresses (t_n^o, t_s^o, and t_t^o), and either the final separation values (δ_n^f, δ_s^f, and δ_t^f) or the fracture energy values (GC_n, GC_s, and GC_t). The properties correspond to each failure mode: normal, shearing, and tearing. These properties were taken from experiments done by Ritter et al. (2009) and are summarized in Table 2.

Table 2. Cohesive interaction properties adapted from Ritter et al. (2009).

Mpa/mm	K_{nn}	150,000
	K_{ss}	150,000
	K_{tt}	150,000
MPa	t_n	68.6
	t_s	10.3
	t_t	68.6
MPa-mm	GC_n	0.075
	GC_s	0.62
	GC_t	0.547

3.3 Double Lap Shear Testing (DLS)

This section presents in more detail the experiments and FEM to predict the interface delamination of FRP composites. A double lap shear (DLS) testing finite element analysis (FEA) performed by Yang et al. (2011) was validated with experimental data from Ritter et al. 2009. In this research, two epoxy temperatures (23°C and 60°C) were considered to study the effect of temperature on the joint and interface failure modes. The DLS specimen configuration is in accordance with ASTM D3528, Type A (ASTM International 2016). Researchers from this study found that the failure mode when using epoxy at 23°C was in the interface of the FRP composite, whereas at 60°C, failure was cohesive within the epoxy. Similar failures were obtained in the experiments and FE models. Refer to Ritter et al. (2009) and Yang et al. (2011), respectively. Results from the DLS test were used to later predict the behavior of more complex structures.

The DLS test FEM was replicated at CERL to verify the capabilities of the traction-separation law when predicting interface delamination. Epoxy properties were studied and compared with the results obtained from the literature for the experiments E13, E14, and E15 by Ritter et al. (2009) and the FEM from Yang et al. (2011), respectively. Three cases were evaluated for the input of the epoxy properties at 60°C and are shown in Figure 5. The same cohesive interaction properties were used for the three cases, while the way the epoxy properties were input was changed. The first case considers the epoxy effective stress-strain curve obtained from the experiments. The second and third cases consider the input of the epoxy properties by defining a slope using two points up to 10.37 MPa (1.50 ksi) and 12 MPa (1.74 ksi), respectively.

Figure 6 shows the load-deflection results of the FEM replicated at CERL versus the experiments and FE models taken from Ritter (2009) and Yang (2011), respectively. Similarly, another case was created for the input of the epoxy properties at 23°C. Load-deflection and failure modes results obtained at CERL were in good agreement with the experiments and FE models from literature. These types of properties and modeling approaches will be used in later chapters.

Figure 5. Epoxy properties cases taken from Ritter et al. (2009) and Yang et al. (2011).

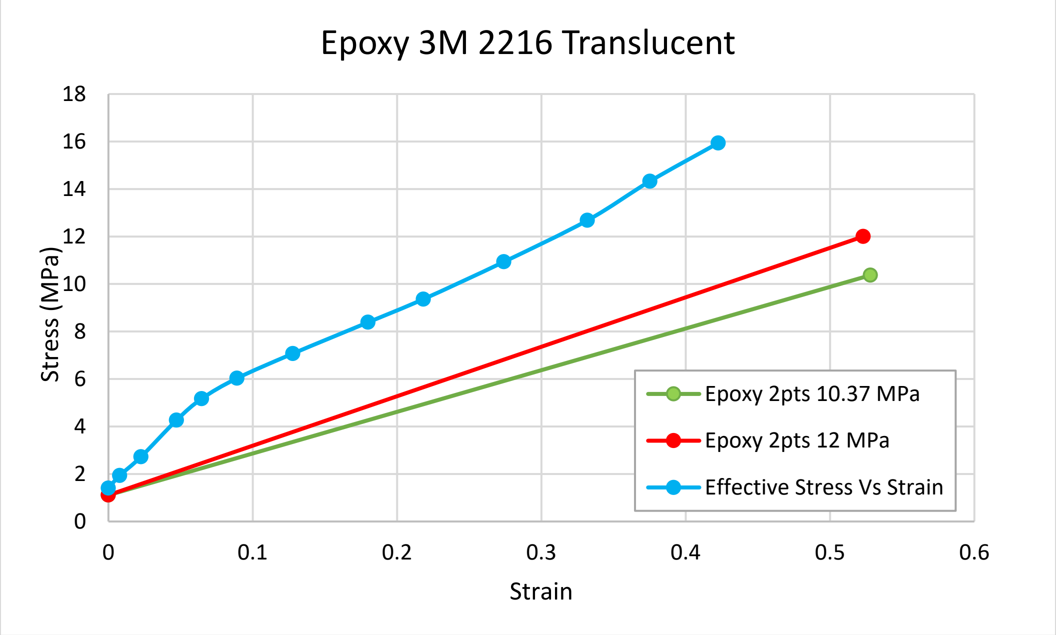

Figure 6. FE models replicated at CERL versus experiments and FE models taken from Ritter et al. (2009) and Yang et al. (2011), respectively.

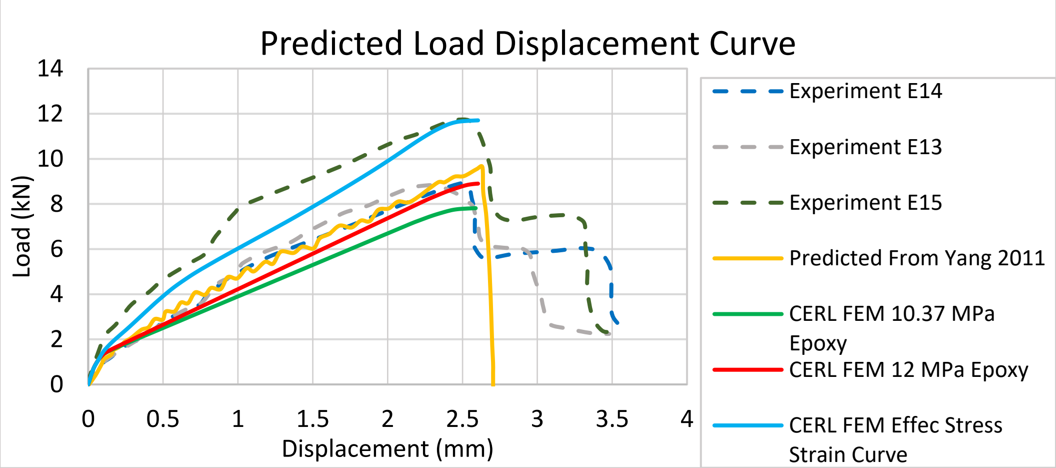

4 Barge Impacts

4.1 Introduction

Since there is no data available in the literature from experiments or FE models related to barge impacts on composite materials, this chapter includes a literature review that summarizes typical barge impact force time histories previously studied by USACE. This report considers typical barge velocities and approach angles according to Engineer Technical Letter (ETL) 1110-2-563 (USACE 2004) and typical barge impact loads obtained from EM 1110-2-2703 (USACE 1994). Information from this chapter will be used as a starting point for the dynamic FEA on FRP composite sandwich panels discussed in Chapter 6.

4.2 Full-Scale Field Test

According to Table A.1 in (Ebeling et al. 2010), a glancing-blow impact event of a barge train affecting an approach wall is an event of less than four seconds. The contact time between the impact corner of the barge train and the approach wall can be as short as a second or as long as several seconds. Researchers such as Patev, Barker, and Koestler (2003b) and Ebeling et al. (2010) found that the duration of contact during impact by the 2-by-2 barge train with the stiff-to-rigid wall at Old Lock and Dam 2 to have a mean impact time of 3.05 seconds with a standard deviation of 0.34 seconds (coefficient of variation [COV] of 0.11). Scaling of an existing impact force time history recorded at the full-scale field tests conducted at Winfield Lock and Dam by Ebeling et al. (2010) is shown in Figure 7.

Figure 7. Scaling of an existing pulse force time history recorded at the full-scale impact experiment conducted at Winfield Lock and Dam by Ebeling et al. (2010). (Public domain.)

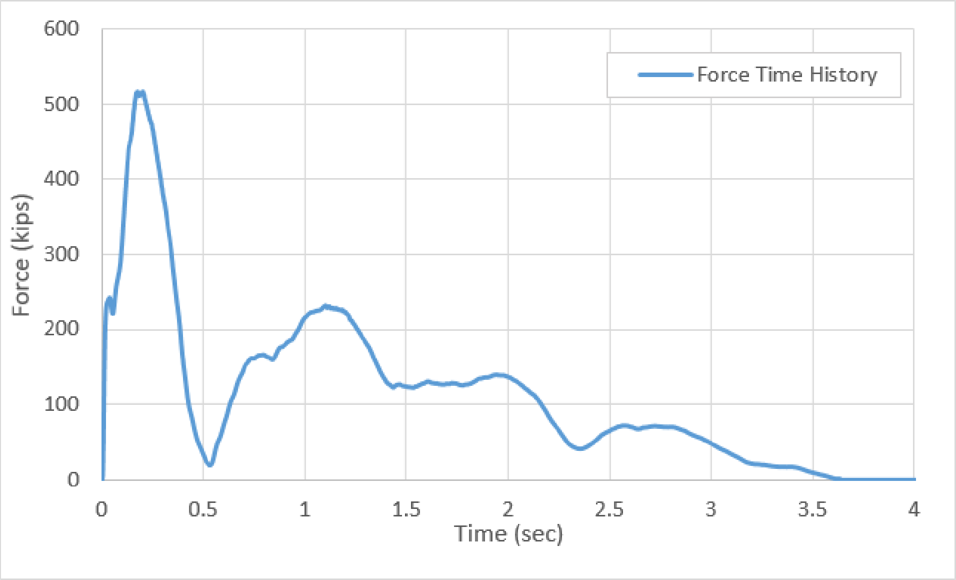

4.3 Typical Velocities and Approach Angles

Information from Table B-3 of ETL 1110-2-563 is provided to illustrate the impact angles as well the range of non-site-specific forward velocities (V_X) and lateral velocities (V_Y) of a barge train for usual, unusual, and extreme barge impact events (USACE 2004). The Table B-3 information from ETL 1110-2-563 is presented in Table 3 (USACE 2004). Dynamic FEA on FRP composite sandwich panels discussed in Chapter 6 will consider “usual” forward velocity conditions to determine barge impact force time histories.

Table 3. Non-site-specific barge impact angles and velocities (USACE 2004).

Load Condition	Approach Angle (θ_X) (degree)	Forward Velocity (V_X) (fps)	Lateral Velocity (V_Y) (fps)
Usual	5–10	0.5–2.0	0.01–0.1
Unusual	10–20	3.0–4.0	0.4–0.5
Extreme	20–35	4.0–6.0	>1.0

Barge train and velocity vector transformation from local barge train to global (wall) axis taken from ERDC/ITL TR-04-2 is shown in Figure 8.

Figure 8. Barge train and velocity vector transformation from local to global axis (Reproduced from Arroyo-Caraballo and Ebeling 2004. Public domain.)

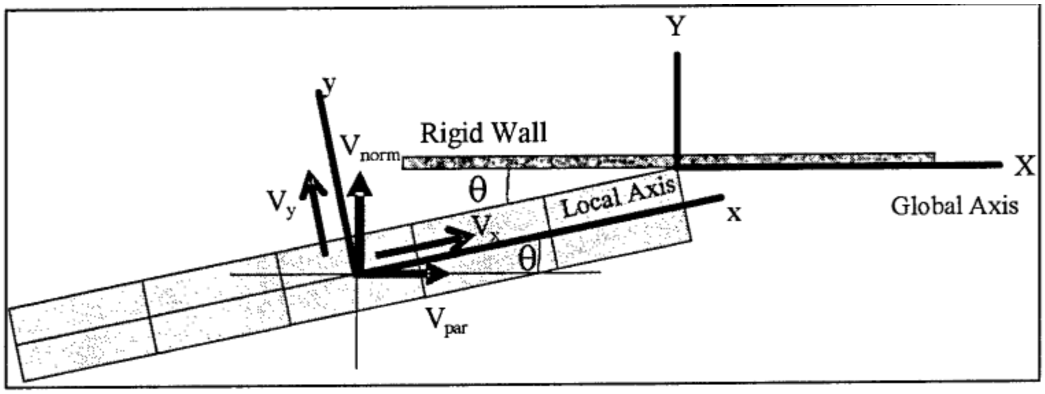

4.4 Typical Impact Loads

According to EM 1110-2-2703, typical barge impact loads for horizontally framed miter gates are classified as symmetric and unsymmetric (USACE 1994). Barge impact loads where the point of load is applied above pool at the miter is a symmetric impact, and anywhere to within 35 ft, the standard barge width, of either lock wall is unsymmetric. Symmetric and unsymmetric impact loads range between 1,112 kN (250,000 lb) and 1,779 kN (400,000 lb), respectively. Similar load ranges were recorded at the full-scale field tests conducted at Winfield Lock and Dam by Ebeling et al. (2010).

5 FRP Composite Sandwich Panels

5.1 Introduction

This chapter presents geometry, material properties, and typical layouts of the FRP composite sandwich panels to be used for the dynamic FEA in Chapter 6. Material properties and geometries as well as angle orientations are discussed for each layer of the laminate. Properties obtained from the product data sheets and assumptions made regarding data not available in the literature are also included.

5.2 Sample Geometry

The FRP composite sandwich panels length, width, and thickness dimensions are 1,828.8 mm (72 in.), 330.2 mm (13 in.), and 152.4 mm (6 in.), respectively. Typical samples dimensions are shown in Figure 9. A typical layup of Section A-A is shown in Table 4.

Figure 9. Sample geometry: (*a*) length and width, (*b*) Section (A-A) thickness, and (*c*) Section (B-B) thickness.

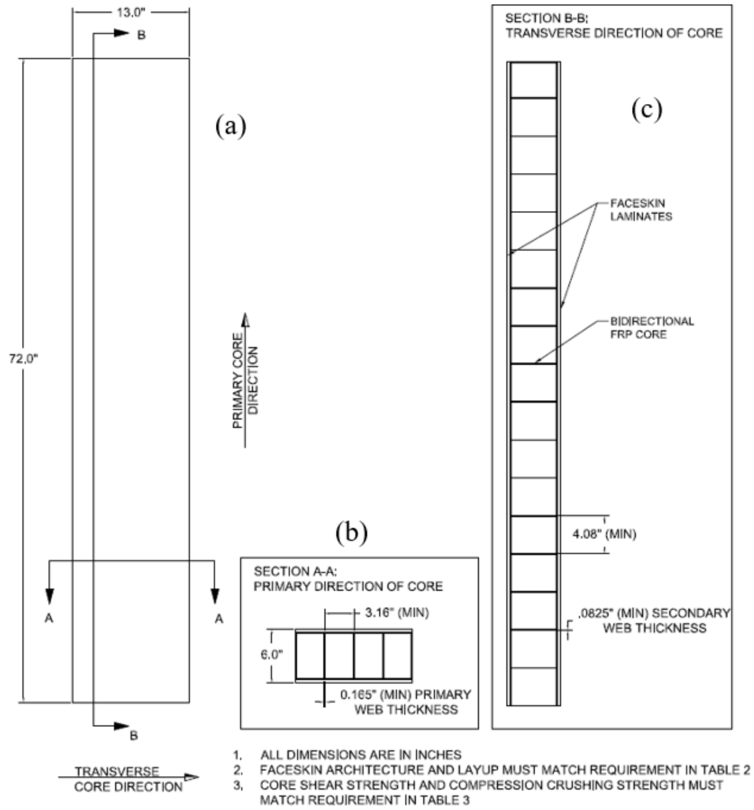

Table 4. FRP composite sandwich panels, typical layup.

Face Skin Layup		Thickness	
Units		in.	mm
E-LT 5500	0 degree	0.054	1.372
E-TTX 4000	0 degree	0.039	0.991
E-LT 5500	90 degree	0.054	1.372
E-TTX 4000	90 degree	0.039	0.991
E-TTX 4000	90 degree	0.039	0.991
E-LT 5500	90 degree	0.054	1.372
E-TTX 4000	0 degree	0.039	0.991
E-LT 5500	0 degree	0.054	1.372
Bidirectional FRP Core			
E-LT 5500	0 degree	0.054	1.372
E-TTX 4000	0 degree	0.039	0.991
E-LT 5500	90 degree	0.054	1.372
E-TTX 4000	90 degree	0.039	0.991
E-TTX 4000	90 degree	0.039	0.991
E-LT 5500	90 degree	0.054	1.372
E-TTX 4000	0 degree	0.039	0.991
E-LT 5500	0 degree	0.054	1.372

5.3 Sample Material Properties

Several materials and angle orientations were used for the FRP composite sandwich panels. The materials used for the face skin are E-LT 5500, and E-TTX 4000. Face skin and core material properties along fiber directions (1) and (2) were obtained from the product data sheets and are summarized in Table 5. In absence of properties along fiber direction 3, properties were assumed equal to properties along fiber direction 2. Poisson's ratios were not available in the product data sheet and were assumed equal to those obtained by experiments at West Virginia University by Vijay et al. (2016).

Table 5. Face skin and core material properties.

E-LT 5500				E-TTX 4000			Bidirectional FRP Core		
Units		tonne/mm^3	kip/in.^{3}	—	tonne/mm^3	kip/in.^{3}	—	tonne/mm^3	kip/in.^{3}
Density	ρ	1.90E-09	6.86E-05	ρ	1.90E-09	6.86E-05	ρ	2.02E-09	7.30E-05
Units		MPa	ksi	—	MPa	ksi	—	MPa	ksi
Young's Modulus along fiber dir 1	E_{11}	45,320	6,573	E_{11}	15,610	2,264	E_{11}	29,649	4,300
Young's Modulus along fiber dir 2	E_{22}	16,830	2,441	E_{22}	24,690	3,581	E_{22}	15,721	2,280
Young's Modulus along fiber dir 3	E_{33}	16,830	2,441	E_{33}	24,690	3,581	E_{33}	15,721	2,280
Poisson's ratio	ν_{12}	0.26	0.26	ν_{12}	0.38	0.38	ν_{12}	0.38	0.38
	ν_{13}	0.26	0.26	ν_{13}	0.38	0.38	ν_{13}	0.38	0.38
	ν_{23}	0.35	0.35	ν_{23}	0.38	0.38	ν_{23}	0.38	0.38
Units		MPa	ksi	—	MPa	ksi	—	MPa	ksi
Shear Modulus in plane 1-2	G_{12}	4,530	657	G_{12}	8,920	1,294	G_{12}	3,406	494
Shear Modulus in plane 1-3	G_{13}	4,530	657	G_{13}	8,920	1,294	G_{13}	3,406	494
Shear Modulus in plane 2-3	G_{23}	4,530	657	G_{23}	8,920	1,294	G_{23}	3,406	494

6 Dynamic Finite Element Analysis (FEA) on FRP Composites Sandwich Panels

6.1 Introduction

Details of the numerical models developed in this investigation are presented in this chapter. To be able to simulate dynamic analyses, the commercially available nonlinear finite element software Abaqus/Explicit was used for this study. The traction-separation law available in Abaqus, and previously discussed in Chapter 3, was used to incorporate cohesive interaction properties to evaluate the damage between FRP composite laminate layers as well as the core separation in the sandwich panels. Force, displacement, and velocity time histories for several masses and velocities representing real-world scenarios were obtained to develop experimental testing procedures for these types of structures.

6.2 Material Properties

Material properties discussed in Chapter 5 were input into the Abaqus/Explict FE model by using the following engineering constants:

- Young’s modulus along fiber direction 1, 2, and 3
- Poisson’s ratios in plane 1-2, 1-3, and 2-3
- shear modulus in plane 1-2, 1-3, and 2-3

In addition, interaction properties as discussed in Chapter 3 were assigned to the model to simulate core damage and interface delamination.

6.3 Boundary Conditions

This section presents the boundary condition (BC) cases considered for the study (See Figure 10). The length and width of the sample were oriented in x and y axes, respectively. Case 1 simulated a simply supported beam, whereas Case 2 simulated the composite sandwich panel resting on a flat surface. These BCs were selected to represent real-world conditions, where Cases 1 and 2 represented a vertical lift gate in the closed condition and miter gates in open condition resting on a concrete wall, respectively. Case 1 is represented as a pin-roller BC with a span length of 1,676 mm (66 in.) between the rollers. Case 2 restrained vertical movement at the bottom face skin and two nodes were selected, as shown in Figure 10, to restrain movement in the other directions for modeling stability purposes.

Figure 10. Boundary conditions (BCs): (*a*) simply supported and (*b*) composite resting on a flat surface.

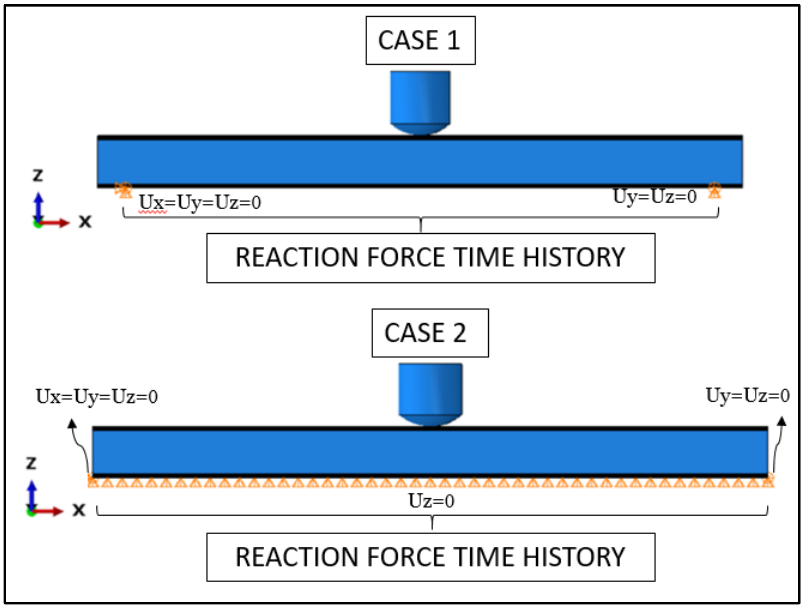

6.4 Plate and Impactor (Rigid Body)

To produce the impact on the composite sandwich panel FE models, two rigid bodies were created for each BC case. The first proof of concept analyses were performed by using a simplified 76.2 mm × 330.2 mm (3 in. × 13 in.) plate impactor. Later analyses incorporated a scaled impactor with a diameter of 170.18 mm (6.7 in.) in order to simulate the leading corner of a barge at forces within the limits of the load frame that was used for validation testing. Results and comparisons are shown for both rigid bodies in later sections of this chapter. The rigid bodies are shown in Figure 11.

Figure 11. Rigid bodies created to produce the impact on FRP composite sandwich FE models.

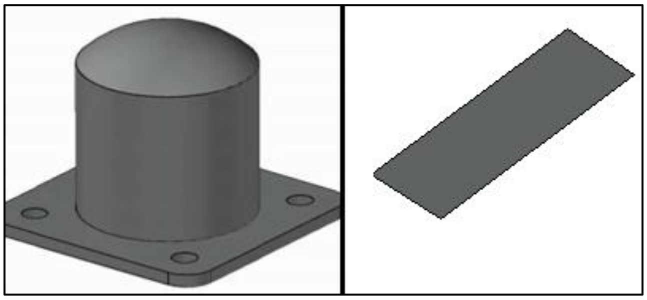

Dimensional analysis was conducted to appropriately scale barge dimensions and mass to this diameter of impactor. Yang et al. (2013) studied the scaling effects in the low-velocity impact response of sandwich structures by using a similar approach to the Buckingham Pi theorem. These researchers summarized in a table the scaling factor "*n*" used to scale dimensions, mass, forces, displacement, among others as shown in Table 6.

Table 6. Impact parameters and scale factor "*n*" taken from Yang et al. (2013).

Parameter	Scaling factor
Panel thickness	n
Diameter of impactor	n
Support ring size	n
Edge length	n
Impact mass	n^3
Impact energy	n^3
Impact contact duration	n
Maximum impact force	n^2
Target displacement	n
Damage area	n^2

A similar approach was used to create the scaled impactor with a diameter of 170.18 mm (6.7 in.) for this research. To determine the full-scale diameter of the corner of a barge, we assumed dimensions of 59.4 m × 10.67 m (195 ft × 35 ft) and found a corner diameter of 0.63 m (2.07 ft), as shown in Figure 12. Since this impactor diameter is larger than the composite sandwich sample to be tested, the impactor diameter was multiplied by the "*n*" factor. This factor was calculated by dividing the composite sandwich sample thickness of 152.4 mm (6 in.) by a typical gate thickness of 558.8 mm (22 in.), such as that of the W. P. Franklin gate. The "*n*" factor was 0.2727. This same factor will be used in the following sections to calculate the scaled mass to be used in FE models.

Figure 12. Impactor dimensions obtained by assuming impact at a 195 ft × 35 ft barge corner.

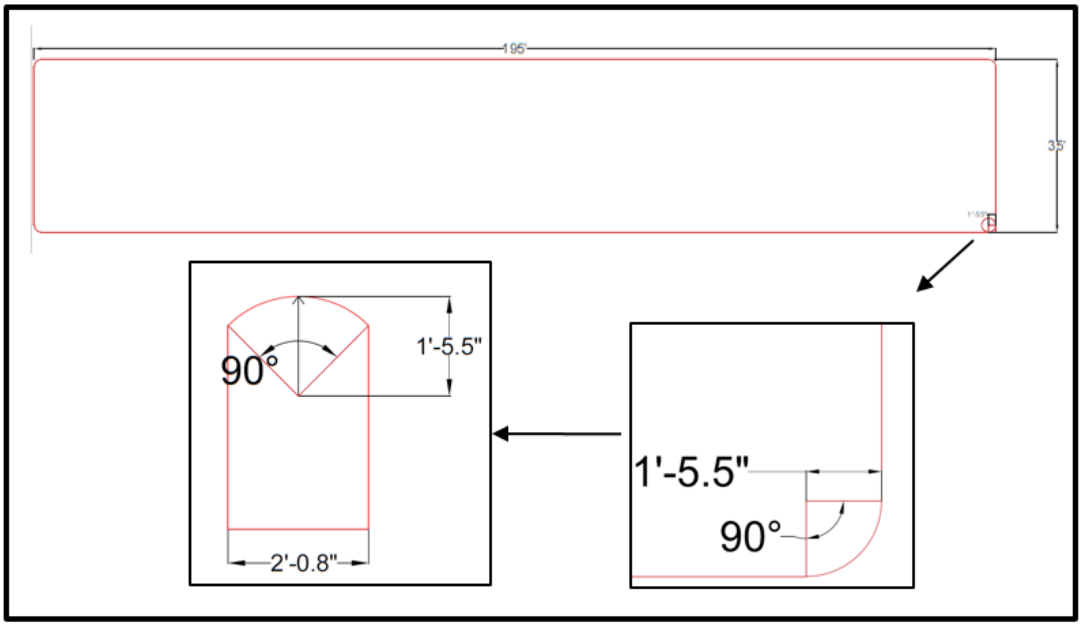

6.5 Mass and Initial Velocity

Mass and initial velocity cases are discussed in this section. Several mass and initial velocity cases were applied by creating a reference point and attaching it to the rigid body. Each mass and velocity case was evaluated for both BC cases, as shown in Figure 13.

Figure 13. Mass and initial velocity to be studied for each BC case.

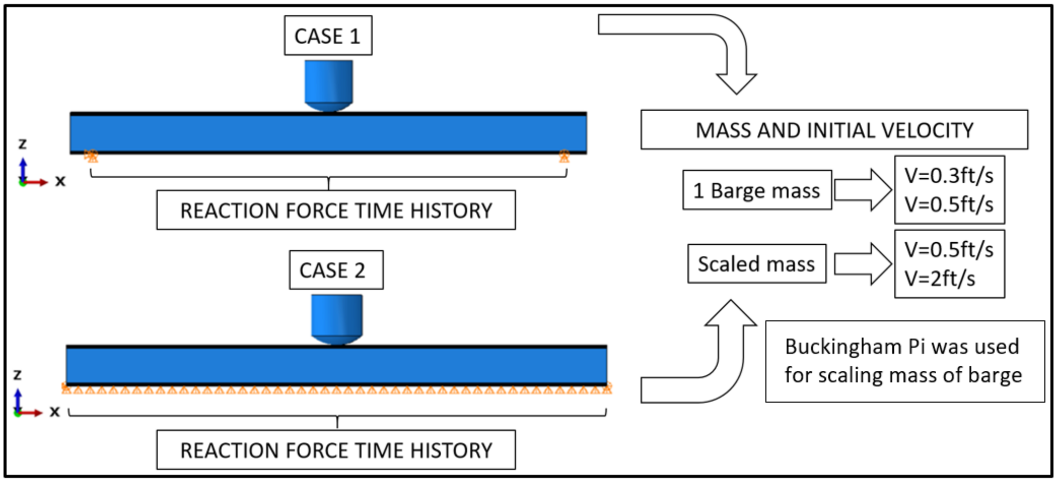

Typical barge mass was obtained from the 1998 full-scale, low-velocity, controlled barge impact experiments conducted at the decommissioned Gallipolis Lock at Robert C. Byrd Lock and Dam. The total weight per barge was approximately 1,940 tonnes (3,880,000 lb). In addition, a tow weight of 550 tonnes (1,100,000 lb) was considered. To include hydrodynamic added mass, a factor of 1.05, as described in equation 2-3 and 2-4 of ETL 110-2-338 (1993), was multiplied by the mass of both barge and tow, respectively. The total mass for one barge, the tow, and the hydrodynamic added mass was 2,369,923 kg (162,391 slug). The obtained mass was input in the FE model as 2,369.923 tonnes, and later scaled to 48.06 tonnes (3,293.16 slug) by multiplying the full mass by the “n^3” factor shown in Table 6. Results will be presented for both mass cases as well for velocity cases ranging in the “usual” interval from Table 3.

6.6 Results

This section presents the numerical models results for each BC case. Several time histories were obtained for the mass and velocity cases discussed in the previous section. In addition, von Mises stress comparison for the impacts when using the plate and impactor rigid bodies is presented in this section.

Time history results for the impact produced by the plate rigid body are summarized in Figures 14 and 15, for the simply supported (Case 1) and resting on flat surface (Case 2) BCs, respectively. A force time history comparison between BCs is shown in Figure 16.

Figure 14. Force time history for scaled mass (SM) and barge mass (BM)—Case 1 BC.

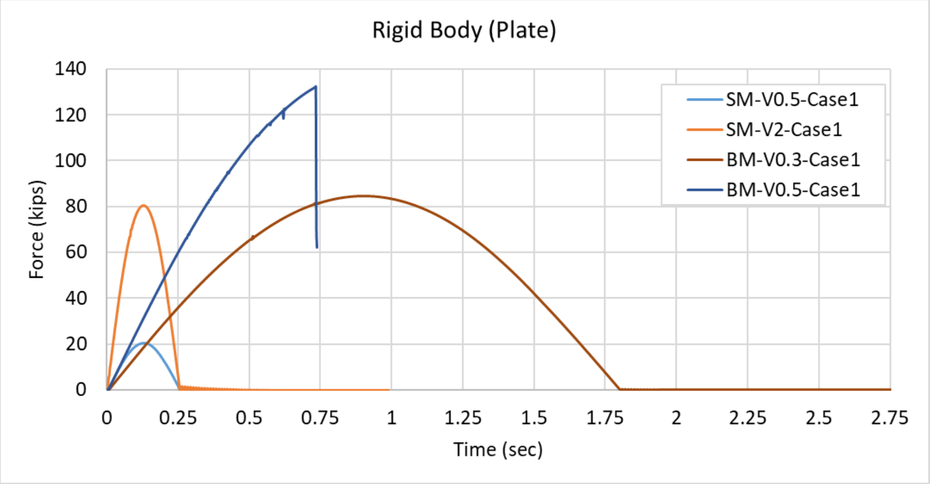

Figure 15. Force time history for SM and BM—Case 2 BC.

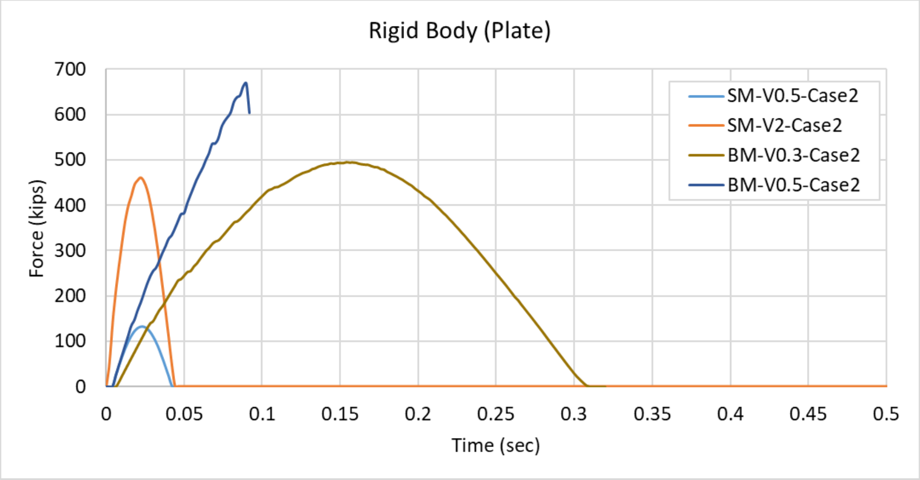

Figure 16. Force time history for SM—Case 1 BC versus Case 2 BC.

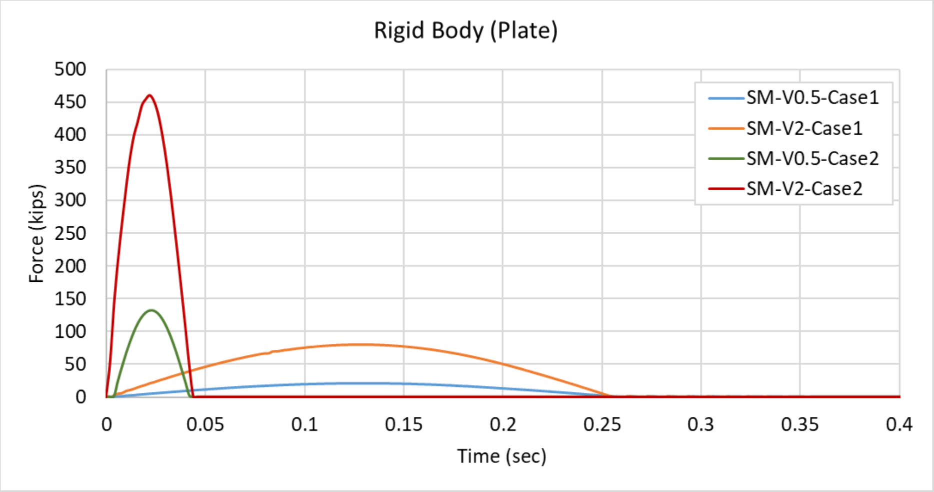

These results provide the following information:

- When using the same initial velocity, the force time history slope will be the same, and the peak load will increase or decrease depending on the mass of the rigid body. If the mass increases, then the peak load will also increase (See Figure 14 and Figure 15).
- When using the same mass, peak load will be approximately scaled proportionally with the velocity. If the velocity increases by a factor of 4, the peak load will similarly be 4 times higher (See Figure 14).
- When comparing both cases of BC, the simply supported Case 1 requires more time for force to return to zero, whereas the composite resting on a flat surface (Case 2) takes less time but produces higher reaction forces (See Figure 16).

A comparison of time history results for the impact produced by the two rigid bodies, the plate and impactor respectively, is summarized in Figures 17 and 18. No major differences in force time history can be seen when comparing the impact produced by the plate versus the impact produced by the impactor for Case 1 BC. The force time history produced by the impactor tends to show lower reaction force while taking more time to reach the peak and decrease back to zero as shown in Figure 17.

Figure 17. Force time history for plate versus impactor rigid bodies—Case 1 BC.

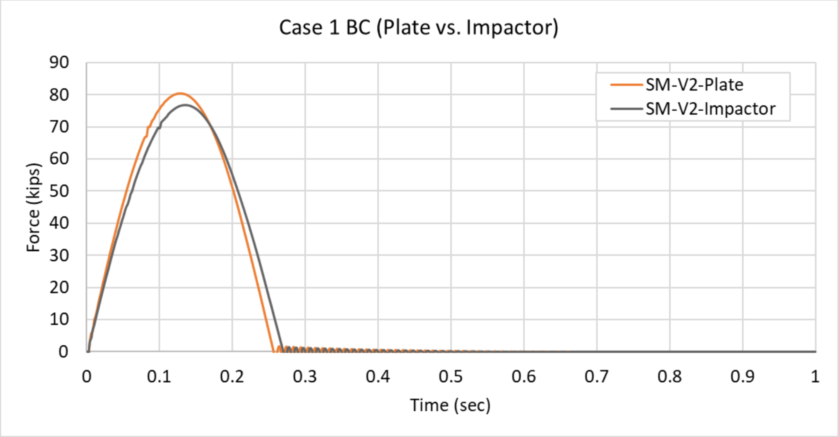

However, several differences in force time history can be seen when comparing the impact produced by the plate versus the impact produced by the impactor for the Case 2 BC, as shown in Figure 18*a*. When using the impactor, the displacement on the top surface of the FRP composite sandwich panel is greater than when using the plate (see Figure 18*b*). Similar behavior is shown for both velocity cases when using the scaled mass (SM). Even greater displacement and deformation can be seen when using the mass equivalent to one barge.

Figure 18. Plate versus impactor: (*a*) force time history and (*b*) displacement time history—Case 2 BC.

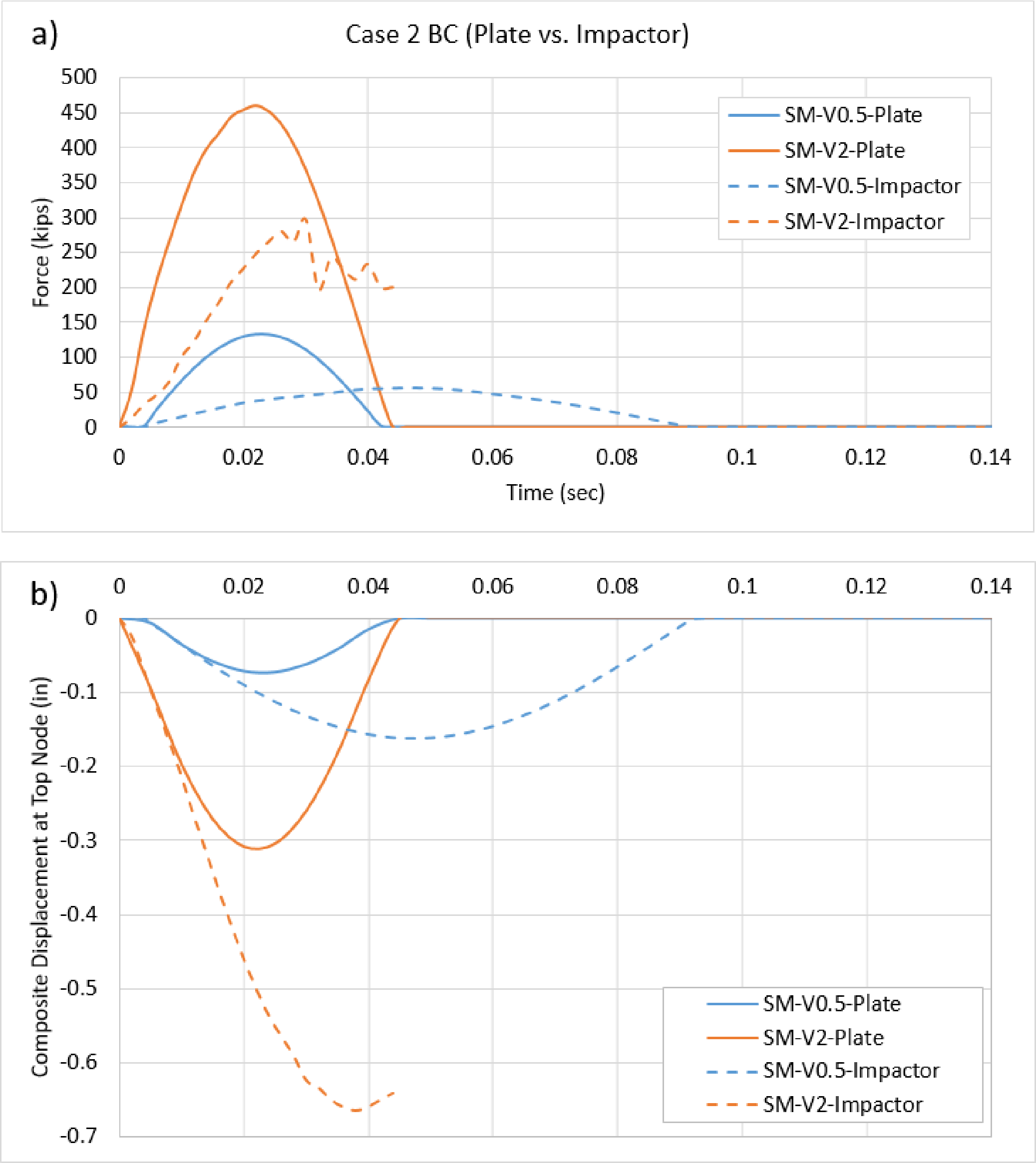

A von Mises stress megapascal (MPa) comparison of the impacts when using the plate and impactor (*left* and *right*, respectively) is shown in Figure 19. The von Mises stress diagrams represent an impact using a scaled mass and initial velocity of 0.5 ft/sec (SM-V0.5) at the time of 0.03 sec. In addition, a top-view comparison is shown (*bottom* of the image). From this comparison, we find that when using the plate, the impact is distributed across the primary and secondary webs uniformly, whereas when using the impactor, the impact is more concentrated. The impactor therefore produces higher stresses and displacements on the top face skin. This behavior is more pronounced in Case 2 BC than in Case 1 BC due to the bottom of the composite panel resting on a flat surface not being able to experience global vertical displacement, which produces more deformation on the top face skin.

Figure 19. Von Mises stress comparison plate versus impactor for scaled mass and initial velocity of 0.5 ft/sec (SM-V0.5)—Case 2 BC.

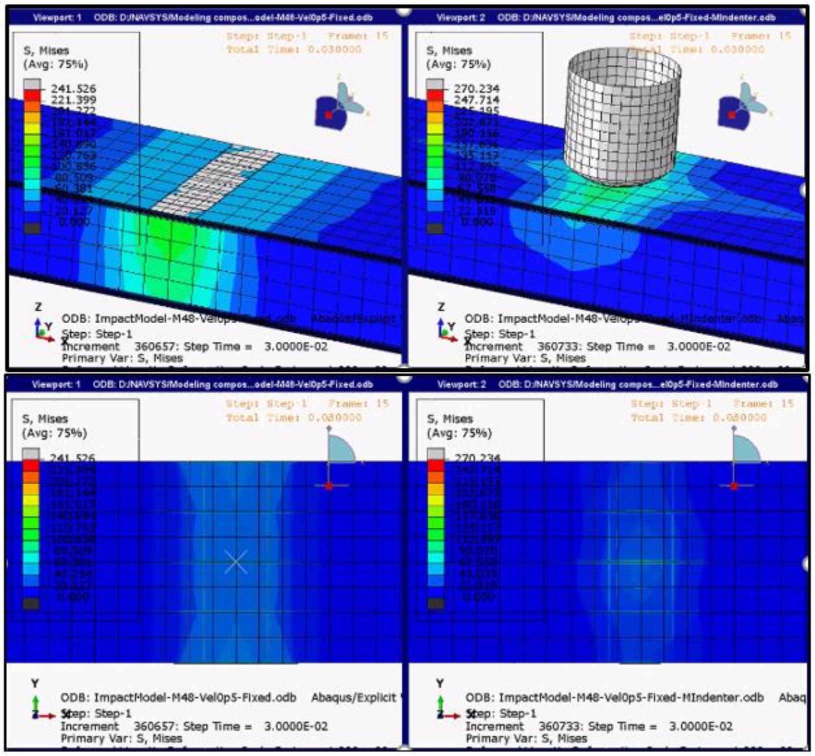

ODB: ImpactModel-M48-Vel0p5-Fixed.odb Abaqus/Explicit
Step: Step-1
Increment 360657: Step Time = 3.0000E-02
Primary Var: S, Mises

ODB: ImpactModel-M48-Vel0p5-Fixed-MIndenter.odb Abaq
Step: Step-1
Increment 360733: Step Time = 3.0000E-02
Primary Var: S, Mises

Force time histories obtained with FE models using the impactor are shown for each BC case in Figure 20. Case 2 BC time histories obtained with an FE model show the worst-case scenario and will be used to experimentally produce several impacts on the FRP composite sandwich samples. Note that as opposed to the plate, where the peak load scales linearly with the velocity, the peak load scaling with the impactor seems not necessarily linear.

Figure 20. Force time histories to be used on experimental testing: (*a*) Case 1 BC and (*b*) Case 2 BC—impactor.

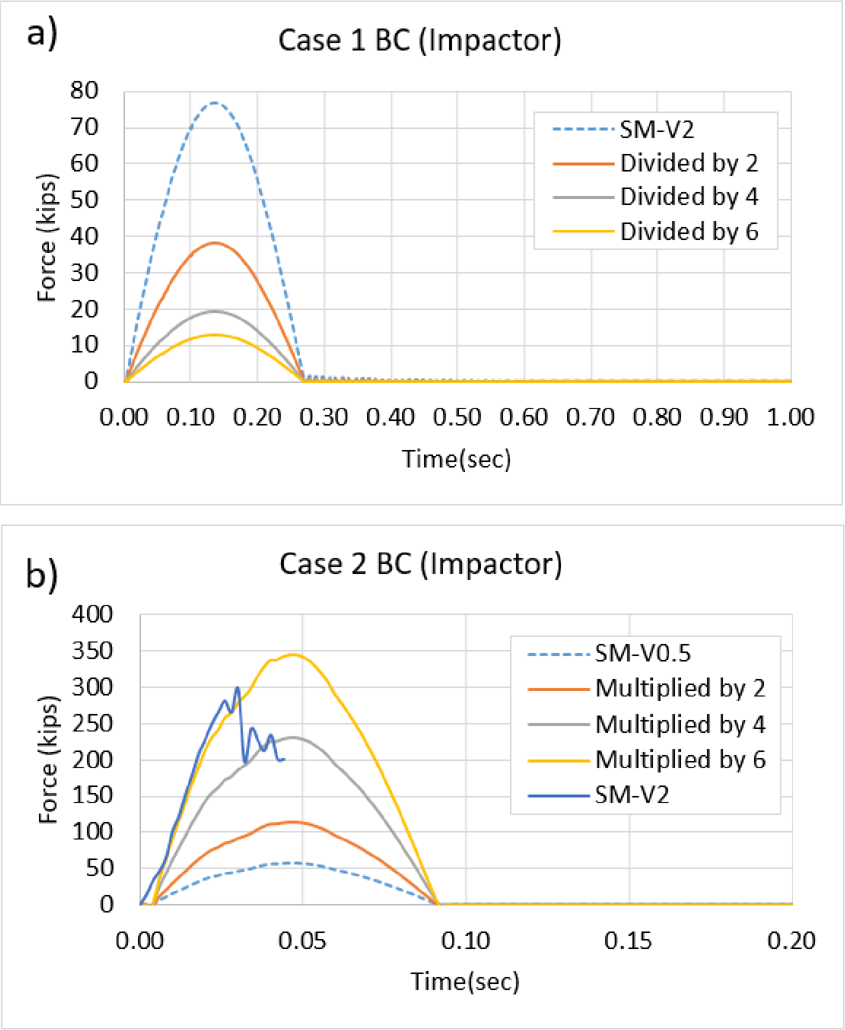

7 Conclusions and Recommendations

A summary of conclusions and recommendations drawn from the experimental results and our observations follows:

- FE models with orthotropic properties can achieve very good predictions when using engineering constants available in Abaqus software.
- The traction-separation law available in Abaqus seems to be suitable when predicting interface delamination of FRP composite sandwich structures.
- When using the same initial velocity, the force time history slope will be the same and the peak load will increase or decrease depending on the mass of the rigid body. If the mass increases, then the peak load will also increase.
- When using the same mass, the peak load will be approximately scaled as much as the velocity. If the velocity increases by a factor of 4, the peak load will similarly be 4 times higher.
- When comparing rigid body BC cases (simulating the closed condition of a vertical lift gate versus an open miter gate resting on flat surface), the closed condition case of a vertical lift gate is subjected to a lower force and takes more time for the force to return to zero, whereas the rigid body resting on a flat surface, such as a miter gate in recess, takes less time to recover but produces higher reaction forces.
- When using an impactor rather than a plate, the FRP composite sandwich panel top displacement is higher. Plate impact is distributed across the primary and secondary webs uniformly, whereas when using the impactor, the impact is more concentrated, producing higher stresses and displacements on the top face skin.
- Time histories obtained with the FE model for the BC case of a FRP composite sandwich panel resting on flat surface present the worst-case scenario. Hence, this case will be used to experimentally produce several impacts on the FRP composite sandwich samples.
- Force time histories obtained in this research will be used as a starting point for the experiments and will be adapted depending on CERL's million pounds frame capabilities.

Bibliography

Abaqus-2017, 2017. *Abaqus 2016 User Documentation—User Manual*. Providence, RI: Dassault Systèmes Simulia Corp.

Arroyo-Caraballo, J. R., and R. M. Ebeling. 2004. *A Numerical Method for Computing Barge Impact Forces Based on Ultimate Strength of Lashings between Barges*. ERDC/ITL TR-04-2. Vicksburg, MS: Information Technology Laboratory.

ASTM International. 2016. *Standard Test Method for Strength Properties of Double Lap Shear Adhesive Joints by Tension Loading*. D3528-96. West Conshohocken, PA: ASTM International.

Ebeling, R. M., B. C. White, A. N. Mohamed, and B. C. Barker. 2010. *Force Time History During the Impact of a Barge Train with a Lock Approach Wall Using Impact_Force*. EDRC/ITL TR-10-3. Vicksburg, MS: Information Technology Laboratory.

Patev, R. C., B. C. Barker, and L. V. Koestler. 2003. *Prototype Barge Impact Experiments, Allegheny Lock and Dam 2, Pittsburgh, Pennsylvania*. ERDC/ITL TR-03-2. Vicksburg, MS: Information Technology Laboratory. http://hdl.handle.net/11681/10956.

Ritter, G. W., D. R. Speth, and Y. P. Yang. 2009. "Qualifications of Adhesives for Marine Composite-To-Steel Bonded Applications." *Journal of Ship Production and Design* 25 (4): 198–205. https://doi.org/10.5957/jsp.2009.25.4.198.

USACE (US Army Corps of Engineers). 1994. *Lock Gates and Operating Equipment*. Engineer Technical Letter (ETL) 1110-2-2703. Washington, DC: US Army Corps of Engineers.

USACE (US Army Corps of Engineers). 2004. *Barge Impact Analysis for Rigid Walls*. ETL 1110-2-563. Washington, DC: US Army Corps of Engineers.

Vijay, P. V., P. R. Soti, H. V. S. GangaRao, R. G. Lampo, and J. D. Clarkson. 2016. "Design and Evaluation of an Integrated FRP Composite Wicket Gate." *Composite Structures* 145:149–161. https://doi.org/10.1016/j.compstruct.2016.01.093.

Yang, F. J., M. Z. Hassan, W. J. Cantwell, N. Jones. 2013. "Scaling Effects in The Low Velocity Impact Response of Sandwich Structures." *Composite Structures* 99:97–104. https://doi.org/10.1016/j.compstruct.2012.11.011.

Yang, Y. P., G. W. Ritter, and D. R. Speth. 2011. "Finite Element Analyses of Composite-To-Steel Adhesive Joints." *Advanced Materials and Processes* 169 (6): 24–28.

Abbreviations

BC	Boundary condition
BM	Barge mass
CERL	Construction Engineering Research Laboratory
COV	Coefficient of variation
DLS	Double lap shear
ETL	Engineer Technical Letter
FE	Finite element
FEA	Finite element analysis
FEM	Finite element modeling
FRP	Fiber-reinforced polymers
S4R	A 4-node doubly curved thin or thick shell, reduced integration, hourglass control, finite membrane strains.
SM	Scaled mass
USACE	United States Army Corps of Engineers

REPORT DOCUMENTATION PAGE

1. Report Date January 2024	**2. Report Type** Final Report	**3. DATES COVERED** **START DATE** FY	**END DATE** FY

4. TITLE AND SUBTITLE

Simulated Barge Impacts on Fiber-Reinforced Polymers (FRP) Composite Sandwich Panels: Dynamic Finite Element Analysis (FEA) to Develop Force Time Histories to Be Used on Experimental Testing

5a. CONTRACT NUMBER	**5b. GRANT NUMBER**	**5c. PROGRAM ELEMENT**
5d. PROJECT NUMBER	**5e. TASK NUMBER**	**5f. WORK UNIT NUMBER**

6. AUTHOR(S)

Anthony Perez-Rivera, Jonathan C. Trovillion, Peter B. Stynoski and Jeffrey P. Ryan

7. PERFORMING ORGANIZATION NAME(S) AND ADDRESS (ES)

US Army Engineer Research and Development Center (ERDC)
Construction Engineering Research Laboratory (CERL)
2902 Newmark Drive
Champaign, IL 61822

8. PERFORMING ORGANIZATION REPORT NUMBER

ERDC/CERL TR-24-1

9. SPONSORING/MONITORING AGENCY NAME(S) AND ADDRESS(ES)

US Army Engineer Research and Development Center (ERDC)
Construction Engineering Research Laboratory (CERL)
Champaign, IL 61822

10. SPONSOR/MONITOR’S ACRONYM(S)

11. SPONSOR/MONITOR’S REPORT NUMBER(S)

12. DISTRIBUTION/AVAILABILITY STATEMENT

Distribution Statement A. Approved for public release: distribution is unlimited.

13. SUPPLEMENTARY NOTES

AMSCO 031391; Funding Account U4375150

14. ABSTRACT

The purpose of this study is to evaluate the dynamic response of fiber-reinforced polymer (FRP) composite sandwich panels subjected to typical barge impact masses and velocities to develop force time histories that can be used in controlled experimental testing. Dynamic analyses were performed on FRP composite sandwich panels using the finite element method software Abaqus/Explicit. The “traction-separation” law in the Abaqus software is used to define the cohesive surface interaction properties to evaluate the damage between FRP composite laminate layers as well as the core separation within the sandwich panels. Numerical models were developed to better understand the damage caused by barge impacts and the effects of impacts on the dynamic response of composite structures. Force, displacement, and velocity time histories were obtained with finite element modeling for several mass and velocity cases to develop experimental testing procedures for these types of structures.

15. SUBJECT TERMS

Barges--Impact testing; Fiber-reinforced plastics; Finite element method; Hydraulic structures; Numerical analysis

16. SECURITY CLASSIFICATION OF:			**17. LIMITATION OF ABSTRACT**	**18. NUMBER OF PAGES**
a. REPORT Unclassified	**b. ABSTRACT** Unclassified	**C. THIS PAGE** Unclassified	SAR	37

19a. NAME OF RESPONSIBLE PERSON	**19b. TELEPHONE NUMBER (include area code)**